International Journal of Hydrogen Energy 216 (2026) 153938

Contents lists available at ScienceDirect

International Journal of Hydrogen Energy

journal homepage: www.elsevier.com/locate/he

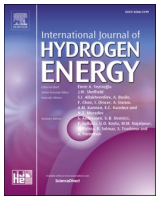

Membrane-integrated process for simultaneous biogas upgrading and hydrogen storage via methanol

Luigi Marsico [a,b], Adele Brunetti [a,*], Enrico Catizzone [b], Massimo Migliori [b], Giuseppe Barbieri [a]

[a] National Research Council – Institute on Membrane Technology "Enrico Drioli" (ITM-CNR), Via Pietro Bucci, Cubo 17C, Rende CS, 87036, Italy
[b] University of Calabria, Chemical Engineering Catalysis and Sustainable Processes Laboratory, Rende CS, 87036, Italy

ARTICLE INFO

Keywords:
E-fuel
Membrane separation
Methanol
Liquid hydrogen carriers
CO_2 valorisation

ABSTRACT

This work presents the design of a membrane-integrated process for biogas valorisation and renewable hydrogen storage via CO_2-to-methanol conversion. The process maximizes CO_2 utilisation by incorporating H_2 from renewable sources, while simultaneously separating methane from biogas to produce a stream suitable for direct injection into the natural gas grid. Membrane units are integrated upstream and downstream of the methanol synthesis reactor: upstream membranes allow to obtain a CO_2-rich stream for methanol production and a CH_4-rich stream compliant with grid specifications, while downstream membranes recover unreacted CO_2 and H_2 for recycling, minimizing emissions and hydrogen losses.

The system is analysed in a step/stage configuration using performance maps from a validated one-dimensional model, accounting for the selectivity and permeance of a polyimide membrane. Results show that biogas can be fully valorised, achieving 98.5% CH_4 recovery with molar purity $\geq$97.5% and ~97% CO_2 conversion to methanol, with nearly complete utilisation of renewable hydrogen. This membrane-integrated approach provides an effective strategy for coupling biogas upgrading with renewable hydrogen storage, enabling sustainable energy storage in the form of methanol e-fuels and contributing to carbon-neutral energy pathways.

1. Introduction

In 2024, global greenhouse gas emissions reached 53.2 $GtCO_2$ equivalent, marking an overall increase of 1.3% compared to 2023 [1]. The larger part of this emissions is given by the CO_2 produced from fossil fuel combustion, which remains the predominant driver of climate change and highlights the urgent need for CO_2 valorisation strategies [2]. In particular, CO_2 emissions have been increasing year-on-year, driven primarily by higher consumption of natural gas, alongside a continued rise in coal and oil usage [3]. The power sector, mainly related to electricity generation, remained the largest source of global greenhouse gas emissions, accounting for approximately 15.5 $GtCO_2e$/year. This was followed by the transport sector, which emitted 8.3 $GtCO_2e$, and by agriculture and industry, each contributing around 6.5 $GtCO_2e$ [1].

The urgency of reducing greenhouse gas emissions necessitates the development of strategies that promote the integration of renewable energy generation into existing infrastructures. One of the sources is biogas, produced via anaerobic digestion from the organic fraction of municipal solid waste, agroforestry residues, and solid waste [4], mainly composed by 50-70% of CH_4, 35-50% of CO_2, small amounts of N_2, O_2, and contaminants as H_2S, siloxanes, and volatile organic compounds [5].

The biomethane obtained by biogas upgrading is a versatile renewable energy that can be utilized across multiple sectors, including electricity generation, heating, and transportation [6]. Owing to its potential to reduce fossil fuels usage and mitigate methane emissions from organic waste streams, such as agricultural residues, manure, and municipal solid waste, it is often considered a carbon-neutral or even carbon-negative energy source [7]. As mentioned, prior to injection into the natural gas grid, raw biogas must undergo an upgrading process to increase its methane concentration and remove impurities. Various

This article is part of a special issue entitled: EFCHC25 conference (Iulianelli) published in International Journal of Hydrogen Energy.

* Corresponding author.
E-mail address: adele.brunetti@cnr.it (A. Brunetti).

https://doi.org/10.1016/j.ijhydene.2026.153938
Received 24 November 2025; Received in revised form 12 January 2026; Accepted 6 February 2026
Available online 10 February 2026

technologies are currently used at the industrial scale for this purpose; among these, membrane separation is particularly effective for separating CH_4 from CO_2, ensuring the production of high-purity biomethane suitable for grid injection and end-use applications [8]. The membrane technology represent an advanced and energy-efficient gas separation technology, providing a viable alternative to conventional separation processes [9]. Membrane also guarantees compact design and operational simplicity, low energy requirements, and lower capital and operating costs, thus offering both economic and environmental benefits [10]. The choice of membranes to be used for the separation depends on the target gas species, the operating temperature as well as the desired purity and recovery levels. For instance, polymeric membranes (polyimide, polisulfone, etc.) are usually used in biogas upgrading [11,12]. Appropriately configured in multistage membrane steps/stages, can simultaneously achieve high product purity and recovery, even when employing membranes with moderate selectivity [12,13]. Membrane separation has also proven to be an effective technology for the selective recovery of CO_2 and H_2 from syngas [14,15]. Recently, Marsico et al. [16] proposed a multi-step membrane separation of a methanator downstream using commercial polyimide membranes, demonstrating that this strategy enhances the valorisation of CO_2 and H_2 utilisation, thereby increasing the overall production of synthetic methane.

Biogas also represents a significant source of biogenic CO_2 produced as a by-product of anaerobic digestion. In addition to carbon capture and storage technologies, carbon dioxide utilisation is considered a readily applicable option in the short to mid-term [17]. Biogenic CO_2 can be converted into valuable products such as fuels, like methanol or methane, and chemicals [18]. Methanol can be produced by the hydrogenation of CO_2 with green hydrogen (Eq. (1)). Additionally, at higher temperatures, the reverse water gas shift reaction can take place (Eq. (2)).

$$CO_2 + 3H_2 \rightleftharpoons CH_3OH + H_2O \tag{1}$$

$$CO_2 + H_2 \rightleftharpoons CO + H_2O \tag{2}$$

The operating conditions of the process are a temperature range of 200–300 °C, a pressure of 40–100 bar. The catalysts generally used are Cu-based catalysts [19]. Methanol ranks among the most extensively utilized chemicals globally, with its demand expected to reach around 120 million tons by 2025 [20]. It represents one of the most versatile platform chemicals in the chemical industry, serving as a key feedstock for the production of acetic acid, formaldehyde, methylamines, methyl *tert*-butyl ether (MTBE), dimethyl ether, and several other derivatives [21]. Beyond its conventional uses, methanol synthesis is increasingly recognised as a one of the most promising candidates for large scale application of carbon dioxide utilisation and effective route for the chemical storage of hydrogen produced from renewable energy surpluses [22]. When produced from biogenic CO_2 and renewable hydrogen, methanol can act both as an energy carrier and as a carbon-neutral fuel, offering the advantage of a higher volumetric energy density compared to hydrogen. This characteristic makes it particularly attractive for hard-to-abate sectors such as aviation and maritime transport, while enabling the coupling of the power sector with the mobility and chemical industries [19]. At the industrial level, efforts have increasingly focused on the use of renewable energy and CO_2 for methanol production, given its potential to mitigate carbon emissions. A pioneering industrial-scale facility is the George Olah Renewable Methanol plant, constructed in 2010-2012 in Svartsengi (Iceland) by Carbon Recycling International (CRI). It integrated CO_2 from the flue gas of a nearby geothermal power plant with hydrogen produced via water electrolysis, achieving a methanol output of approximately 4000 t/year [23]. More recently, CRI has initiated the construction of a commercial-scale plant in Anyang, China, designed for an annual production capacity of 110,000 t of methanol [24].

Usually, the conversion of CO_2 into methanol is around 20% for a temperature of 250 °C and a pressure close to 30 bar [25]. Also in this case, membrane gas separation can improve the process efficiency, enhancing the methanol production by selectively treating a fraction of the reactor downstream stream that would otherwise be purged, enabling the recovery of unreacted species while removing undesired species. This approach ensures a more effective valorisation of CO_2 and improved utilisation of hydrogen.

The present study aims to demonstrate the effectiveness of integrating membrane gas separation units both upstream and downstream of existing industrial plants, through the analysis of a representative case study involving a methanol synthesis reactor. The integration of membrane gas separation enhances overall process efficiency by enabling the selective recycling of unconverted reactants and the upstream removal of methane. Owing to their scalability, operational flexibility, and high technological readiness level, which minimises operational constraints at large scale, polymeric membranes represent a viable and attractive alternative to conventional separation technologies (e.g., pressure swing adsorption) currently used in industrial processes.In this work, a membrane-integrated process was designed for the production of e-fuels through the valorisation of biogas. Specifically, the process aims to maximize the conversion of CO_2 into methanol, adding H_2 produced from renewables, while simultaneously separating the methane contained in the biogas, thus producing a stream suitable for direct injection into the natural gas grid (Fig. 1). The proposed process integrates membrane separation units both upstream and downstream of the methanol synthesis reactor. The upstream units treat the biogas to generate a CO_2-enriched stream for methanol synthesis and a CH_4-rich stream with a composition compliant with natural gas grid specifications. The downstream membrane units recover unreacted CO_2 and H_2 for recycling to the reactor, thereby minimizing CO_2 emissions and H_2 losses.

2. Methods

A previously validated one-dimensional model [26,27], implemented in DWSIM, was used to analyse the membrane separation process. The model considers multicomponent permeation in a steady-state and co-current configuration; further details are reported in the Supplementary Information.The results of this model provide an immediate reference for assessing the effectiveness of each separation step. The model inputs are the molar fractions of the feed components, the pressure ratio (Eq. (4)), and the membrane selectivity (Eq. (5)). The model outputs are the dimensionless flow rates of the species in the retentate, while additional parameters, such as the permeate flow rates, compositions, and membrane areas, were calculated through post-processing.

The main terms of the model are: the permeation number (Eq. (3)) and the pressure ratio (Eq. (4)). The permeation number is defined as the ratio of the maximum flow rate permeating the membrane and the total flow rate along the module [26]. A unitary value denotes the complete permeation of the most permeable component of the feed through the membrane. The pressure ratio (Eq. (4)) is the ratio between the feed and permeate pressures [26].

$$\theta_i = \frac{Permeance_i \, P_i^{Feed} A^{Membrane}}{F_i^{Feed}}, - \tag{3}$$

$$\phi = \frac{P^{Feed}}{P^{Permeate}}, - \tag{4}$$

The separation properties of the membrane were considered in terms of selectivity, expressed as the ratio of the permeances of the two species (Eq. (5)), and permeance, defined as the permeating flux divided by the transmembrane pressure difference (Eq. (6)) [28].

$$Selectivity_{i,j} = \frac{Permeance_i}{Permeance_j}; - \tag{5}$$

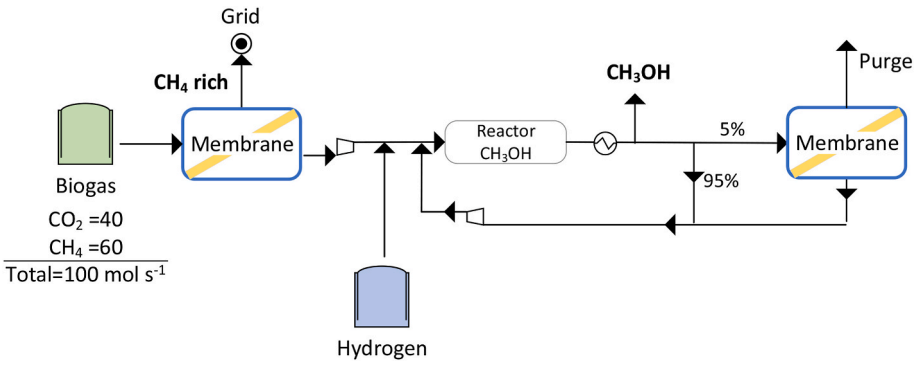

Fig. 1. Scheme of the proposed membrane integrated process.

$$Permeance_i = \frac{PermeatingFlux_i}{Transmembrane\ Pressure\ Difference_i}; mol\ s^{-1}\ m^{-2}\ Pa^{-1} \quad (6)$$

As an input for the model, we considered the selectivities, and the H_2 permeance of polyimide membranes (Table 1), already used for gas separations in industrial applications [26].

Based on the results obtained from the 1D model, the design of the multi-step membrane separation was carried out through the performance maps of the concentration of the single species as a function of its recovery. The adopted model assumes negligible pressure drops within a single module (step). This assumption is justified by the moderate axial flux and by the short module length (<0.5 m). These maps, originally introduced by Brunetti et al. [36], show the concentration of a specific component in the stream as a function of its recovery. For a fixed membrane selectivity and pressure ratio, each curve corresponds to an ideal membrane separation, with every point representing a distinct separation condition. Each point on the map is associated with a permeation number, from which the required membrane area can be determined.

The performance of the membrane separation was assessed by evaluating the performance maps of the recovery of the targeted species in the retentate or permeate stream (Eq. (7)) as a function of the molar composition (Eq. (8)) [38]. Specifically, the recovery in the retentate was considered for less permeable species such as CH_4, while the in the permeate was evaluated for highly permeable species such as H_2 and CO_2.

$$Recovery_i = \frac{Flow\ rate_i^{Retentate/Permeate}}{Flow\ rate_i^{Feed}}; - \quad (7)$$

$$Molar\ composition_i = \frac{Flow\ rate_i^{Retentate/Permeate}}{Flow\ rate_{total}^{Retentate/Permeate}}; - \quad (8)$$

The insights derived from these maps guided the design of the multi-step configuration. This approach enhances membrane separation by dividing a single unit into multiple steps in which the permeate is removed, thereby maintaining a higher driving force between the retentate and permeate sides. Each step consists of a membrane module that receives the retentate stream from the previous one as already compressed feed [13].

Table 1
Properties of polyimide membranes adapted from Ref. [29].

Selectivity, -	
H_2/CO_2	2
H_2/CH_4	90
H_2/CO	45
H_2/H_2O	1
Permeance, nano-mol s^{-1} m^{-2} Pa^{-1}	
H_2	40

The CO_2 valorisation into methanol and the H_2 utilisation were assessed according to Eq. (9) and Eq. (10), respectively. A CO_2 valorisation value of one indicates that all the CO_2 contained in biogas has been valorised into methanol, whereas a value of zero represents no valorisation. Similarly, an H_2 utilisation value of one denotes the complete utilisation of hydrogen, while a value of zero indicates that no hydrogen has been used.

$$CO_2\ valorisation = \frac{Flow\ rate_{CO_2}^{Feed} - \left(Flow\ rate_{CO_2}^{Purged} + Flow\ rate_{CO_2}^{Grid}\right)}{Flow\ rate_{CO_2}^{Feed}}, - \quad (9)$$

$$H_2\ utilisation = \frac{Flow\ rate_{H_2}^{Feed} - Flow\ rate_{H_2}^{Purged}}{Flow\ rate_{H_2}^{Feed}}, - \quad (10)$$

In this study, a CO_2/CH_4 mixture representative of a typical biogas stream was assumed, with molar composition of 40% and 60%, respectively. A molar flow rate of 100 mol s^{-1} was adopted as the calculation basis. As the reactor for methanol production is downstream of a biogas upgrading stage, the CO_2 fed to the reactor results from that coming from the permeate of the membrane stage and the recycle of the reactor downstream. The feed hydrogen flow rate was balanced together with that recycled from the reactor downstream to guaranty a H_2/CO_2 ratio of 3 at the reactor inlet, in accordance with the stoichiometry of the methanol production reaction (Eq. (1) and Eq. (2)). The pressure ratio (Eq. (4)) of the biogas and hydrogen feed streams was set at 20. The CO_2 single-pass conversion to CH_3OH was set at 20%, while the conversion to CO was set to 5% for a temperature of 250 °C [25]. The selected per-pass CO_2-to-CH_3OH conversion is consistent with the 15–25% range as commonly reported in the literature. This limitation arises from the highly exothermic nature of methanol synthesis and its kinetic constraints, as highlighted by Yang et al. [30].As a target for the biomethane purity to be achieved in the biogas membrane separation process, we considered the Italian regulations with a maximum allowable CO_2 concentration in the grid ≤2.5% [42, 43, 44].

The convergence criterion for the steady-state modelling framework in DWSIM was set on the difference in two consecutive iterations of the flow rate of the recycled stream and was stopped when a value lower than 10−12 was obtained.

3. Results and discussion

Fig. 2 depicts the proposed membrane-integrated process for the valorisation of biogas into biomethane and methanol. The feed consists of biogas, with a molar composition of 40% CO_2 and 60% CH_4, and hydrogen derived, for example, from the surplus of renewable electricity [31]. The process delivers two outputs: a biomethane stream at grid-grade purity, and a methanol stream. The integrated system can be conceptually divided into three sections (Fig. 2). The upstream section is devoted to separating methane from CO_2, to obtain an enriched CO_2

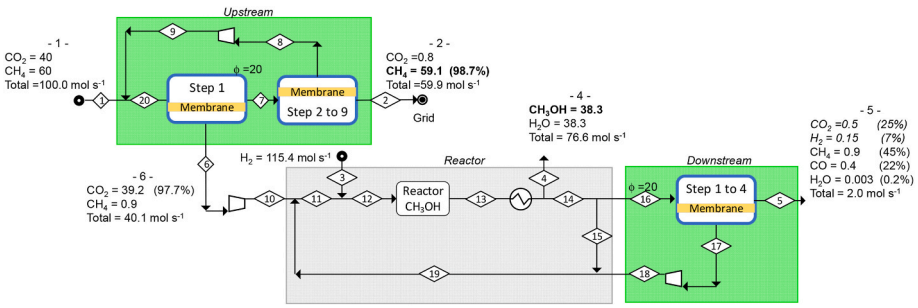

Fig. 2. Membrane-integrated process for the biogas valorisation.

stream to be fed to the reactor and a rich CH_4 stream directly injectable in the grid. The reactor section comprises the reactor itself, which is treated as a black box and not part of this work.The downstream section focuses on the recovery of unreacted H_2 and CO_2 from the reactor purge stream, aiming at maximizing reactant utilisation, enhancing the overall integrated process performance.Table S1–S3 summarise complete mass balances for the various sections of the process reported in Fig. 2.

3.1. Upstream membrane separation

The membrane separation section upstream of the reactor was designed as a single stage comprising 9 steps (Fig. 3). The permeate of the first step, consisting in a CO_2-enriched stream (stream 6) is fed to the reactor. The permeates from the steps following the first one, already containing CO_2 at a lower concentration with respect to the first step (stream 8, with a flow rate of 68.8 mol s^{-1} and a composition of 83 M% CO_2 and 17 M%CH_4), are recycled to the process inlet. This recycling allows methane, which permeates in smaller amounts, to be recycled at the inlet of the separation, thereby increasing its overall recovery. Additionally, the recycling feeds a CO_2-rich stream back to the process inlet, which reflects in an increase of its partial pressure on the feed, thus facilitating its separation. Another advantage of this configuration is that it minimises the amount of methane fed to the reactor section and then the amount to purged. Indeed, since CH_4 does not participate in the reaction, its high concentration within the reactor and the associated recycle loop would negatively impact the overall integrated process performance, particularly considering reactor thermodynamics and kinetics.

The performance of the various steps in terms of CH_4 retentate concentration (Fig. 4a) and CO_2 permeate concentration (Fig. 4b) versus their related recovery is evaluated by developing appropriate performance maps. To facilitate reader comprehension, the discussion is primarily developed with reference to Fig. 4b, which illustrates the behaviour of CO_2 and provides a clearer representation of the curve trends. Nevertheless, the same considerations are equally valid for the case of CH_4 recovered in the retentate.

The analysis was carried out considering a permeation number of 0.5, 1, and 2 (depicted with dotted lines in Fig. 4b) since values close to unity are expected to provide higher separation performance, while the steps are identified by their corresponding numbers. Specifically, at $\theta = 0.5$, lower CO_2 recoveries are achieved along with higher concentrations, whereas at $\theta = 2$, higher recoveries are obtained at the expense of concentration. In the first step, priority was given to the CO_2 concentration at the process outlet by adopting a permeation number of 0.5; in the subsequent steps, a unit value was applied to increase CO_2 recoveries. With this configuration, it was possible to recover 98.5% of the methane contained in the biogas feed stream at the desired purity of 98.7%, highlighted with a green band, and to obtain a CO_2-rich stream with a recovery of 98.1 M% and a purity higher than 97% to be fed to the reactor section. By summing the membrane areas required for each step and considering a total plant feed flow rate of 100 mol s^{-1} (approximately 8200 m^3(STP) h^{-1}), the total membrane area required for the upstream separation is 8848 m^2.

3.2. Downstream membrane separation

From the membrane separation, a permeate stream of 40.1 mol s^{-1} with a CO_2 concentration close to 97.7 M% is fed to the reactor for the production of methanol. At the reactor outlet, methanol and water are completely condensed (Fig. 5, stream 4), whereas the gaseous part of the stream (stream 14) still contains significant amounts of reagents and is recycled at the inlet of the reactor. Nevertheless, the recycle leads to the progressive accumulation of CH_4, which does not take part in the reaction, and CO, which is a secondary product. Consequently, a purge is necessary to avoid the accumulation of these components within the process. The ideal condition under which operating the purge is on maximizing the recycling of H_2 and CO_2, thereby enhancing their utilisation in the integrated process, while removing CH_4 and CO. However, purging a portion of the reactor outlet stream effectively eliminates CH_4 and CO but also results in the undesired loss of valuable reactants, reducing the overall process efficiency. To address this limitation, we proposed a membrane separation unit placed downstream to the reactor after the recycling of part of the stream (Fig. 5). A non-recycled fraction of 5% was selected as a feed for the membrane because it allows a more efficient removal of CH_4 from the reactor, as it will be further discussed in the next section. The selected purge level is selected based on the

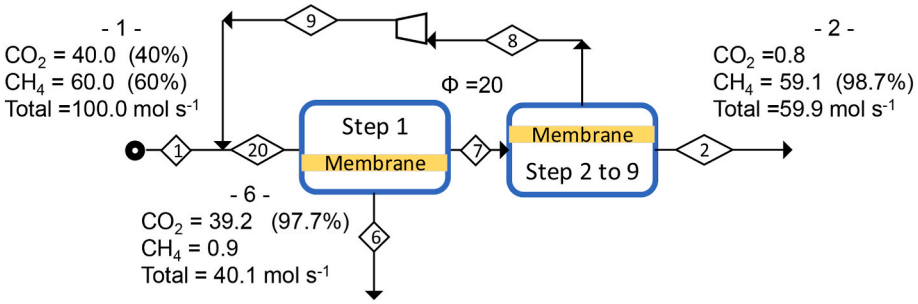

Fig. 3. Upstream membrane separation section.

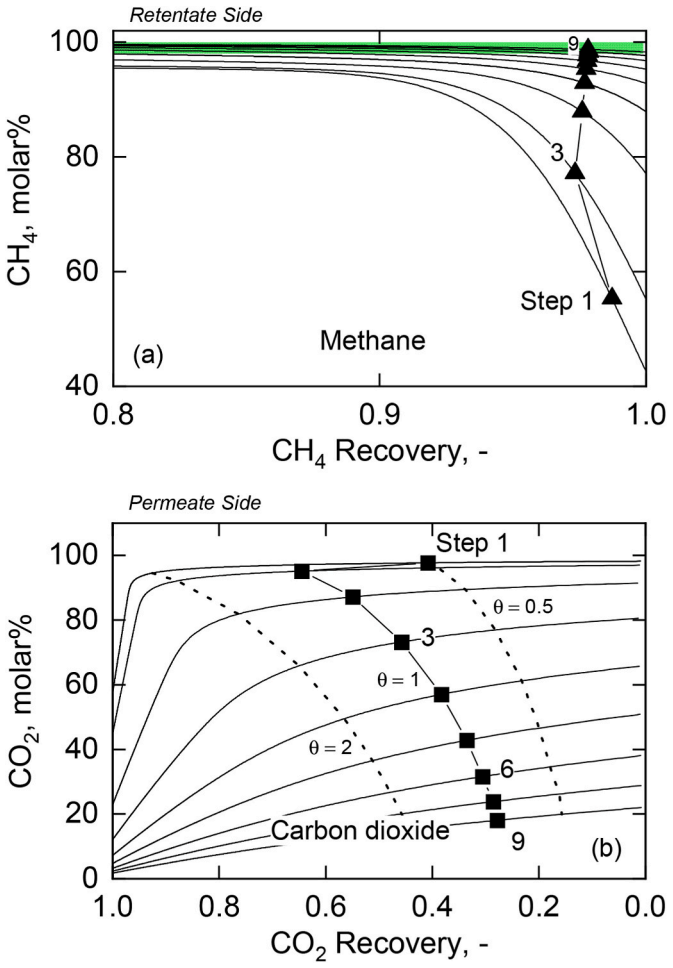

Fig. 4. Performance maps of the retentate and permeate sides of the proposed membrane separation of the biogas stream. The circles and squares on each curve refer to the calculated permeation number selected as most appropriate to achieve the desired separation performance.

fraction of species to be removed. In the investigated process, the reactor outlet stream contains approximately 5% of CO and CH_4. For this reason, a similar percentage of purge stream was used in the simulations. We chose to treat only a fraction of the downstream stream with the membrane unit, as this stream is already rich in reactants (23.4 M% CO_2 and 70.5 M% H_2) owing to the relatively low CO_2 conversion of 20% in the reactor as reported in Table 2.

This membrane separation unit consists of four steps. Each step receives as feed the retentate stream from the previous one, thus avoiding the need for intermediate compression between stages. The feed stream of the membrane process has a total flow rate of 32.52 mol s^{-1} with the remaining part consisting of CH_4, CO, and H_2O (Table 3). As in the previous section, the separation performance of the proposed configuration was analysed by a performance map (Fig. 6). For the membrane process proposed, a unitary permeation number was selected for each step (black dots in Fig. 6b) as this condition ensures a high recovery and concentration of H_2 and CO_2, while preventing the permeation of CH_4 and CO. With a permeation number of 0.5, methane permeation, being less permeable than hydrogen, would be limited. Conversely, at a permeation number equal to 2, CH_4 and CO would also permeate significantly. To facilitate the readers, hydrogen, which is the most permeable species (Table 1), is considered as the first species described.

Since the majority of H_2 permeates the membrane at the initial step, its concentration in the permeate gradually decreases in the subsequent steps. Carbon dioxide, less permeable than hydrogen, increases its concentration in the permeate as the feed stream becomes progressively depleted in H_2. Consequently, the retentate stream (Fig. 6c and d) becomes progressively enriched in CH_4 and CO, which are the less permeable components. Hence, the proposed downstream membrane separation achieves a stream, given by the permeates, with a flow rate of 30.5 mol s^{-1} composed of 23.3% CO_2 and 74.6% H_2 (Table 3), which will be recycled at the inlet of the reactor. The other resulting stream, given by the retentate of step 4 (stream 5 in Fig. 5), purges from the integrated process most of the CH_4 and CO entering the membrane unit. This stream, composed of approximately 74.6% of fuel species (mainly CH_4, H_2, and CO), can be flared or valorised to supply the energy demand of the process. The total membrane area required for the downstream separation process is 600 m^2, a significantly lower value with respect to the upstreams separation section, proportional to a significantly lower feed flow rate.

3.3. Comparison between the configuration with and without membrane separation downstream of the reactor

The proposed configuration, which integrates a downstream membrane separation unit on the purge fraction of the reactor downstream, was compared with the scheme shown in Fig. 7, where we considered a purge of 1%, 3%, or 5%, without introducing membrane separation stages, while stream 15 is recycled to the reactor inlet. The purges considered are consistent with the typical values adopted in industrial methanol production processes [19]. For instance, pilot-plant studies report purge fractions ranging from 2% to 6% of the reactor outlet stream, depending on the fraction of species to be removed [19,32]. Other literature simulation studies also confirm purge fractions in the range of 0.5–5% [33,34]. The purged flow rates obtained from this

Table 2
Input data selected for the simulation of the integrated process.

Flow rate$^{Feed}_{CO_2}$, mol s^{-1}	40
Flow rate$^{Feed}_{CH_4}$, mol s^{-1}	60
CO_2:CH_4 mixture Feed flow rate, mol s^{-1}	100
Flow rate$^{Feed}_{H_2}$, mol s^{-1}	115.4
CO_2 conversion to CH_3OH, %	20
CO_2 conversion to CO, %	5
Membrane separation steps	
Pressure ratio (ϕ), -	20

STP: Standard Temperature and Pressure; 0 °C and 101,325 Pa.

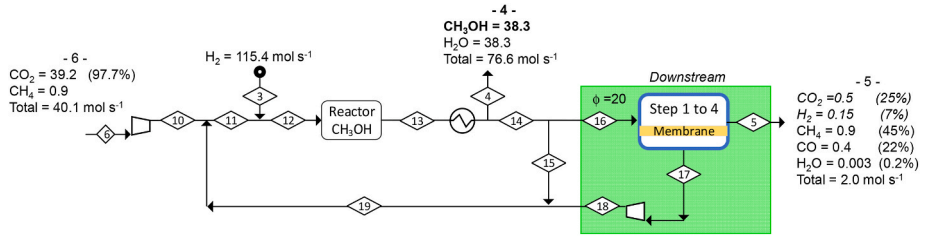

Fig. 5. Downstream membrane separation.

Table 3
Recycled, membrane feed and purged flow rates for the downstream membrane separation proposed process.

	Membrane feed		Permeates (stream 17)		Purged retentate (stream 5)	
	Flow rate, mol s^{-1}	Concentration, molar%	Flow rate, mol s^{-1}	Concentration, molar%	Flow rate, mol s^{-1}	Concentration, molar%
CO_2	7.6	23.4	7.1	23.3	0.51	25.3
H_2	22.9	70.7	22.8	74.6	0.15	7.3
CH_4	1.0	3.0	0.06	0.2	0.91	45.1
CO	0.51	1.6	0.06	0.2	0.45	22.2
H_2O	0.51	1.6	0.5	1.7	0.003	0.2
Total	32.52	-	30.5	-	2.02	-

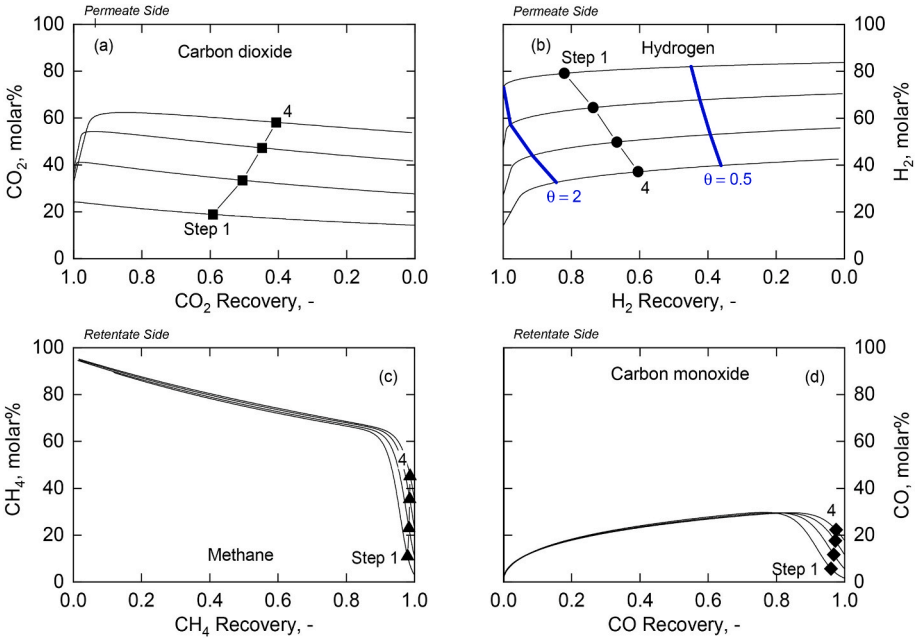

Fig. 6. Performance maps of the membrane unit, which operates on a fraction of the reactor downstream.

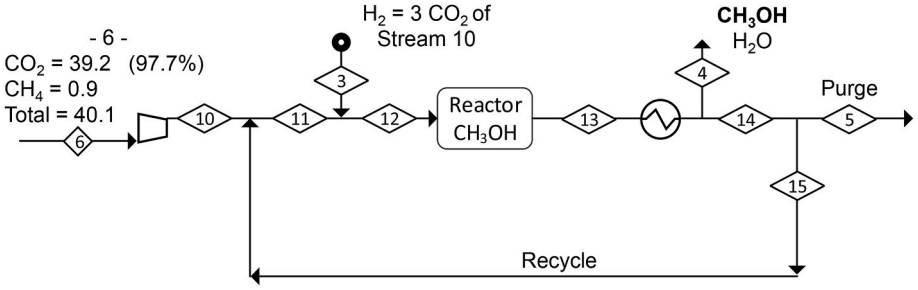

Fig. 7. Integrated process for the valorisation of CO_2 into methanol without membrane separation.

configuration are shown in Fig. 8 - left side. The desired condition is the maximization of the recycling of the CO_2 and H_2 contained in the downstream of the reactor while ensuring the effective elimination of CH_4 and CO. The CO_2 emitted with purging increases from 1.5 to 6.4 mol s^{-1} with increasing purge. Hydrogen exhibits a similar trend, rising markedly from 4.5 to 19.4 mol s^{-1}. It is important to underline that methane flow rate, which does not participate in the reaction, remains constant regardless of the configuration or purge considered; its outlet flow rate is equal to the inlet one (stream 6 in Fig. 7), with a value of 0.91 mol s^{-1}. Carbon monoxide, on the other hand, increases from 0.10 to 0.43 mol s^{-1}, corresponding to approximately 1.5% of the purged stream for all the purges percentages. The addition of the membrane separation on purged stream, shown in blue in Fig. 8 – left side, lead to a significant decrease of the purged reactants, reaching values of 0.51 and 0.15 mol s^{-1} for CO_2 and H_2, respectively. The CO flow rate, with a value of 0.45 mol s^{-1}, is slightly higher than the maximum amount purged in the configuration without membranes.

As expected, an increase in the purged percentage leads to a decrease in the recycled flow rates of the reactant (Fig. 8 - right side), with CO_2 dropping from 149 to 123 mol s^{-1} and H_2 from 447 to 368 mol s^{-1}. However, a higher purged fraction has the beneficial effect of significantly reducing the recycled CH_4 flow rate, from 90 to about 17 mol s^{-1}, along with a decrease in CO from 9.9 to 8.2 mol s^{-1}. Using membrane downstream configuration, 152 mol s^{-1} and 459 mol s^{-1} for CO_2 and H_2, respectively, were recycled which is slightly higher than the best results achieved with 1% purge.

The recycled CH_4 and CO flow rates, equal to 18.5 and 9.7 mol s^{-1}, respectively, are closer to those observed for a 5% purge, which yielded

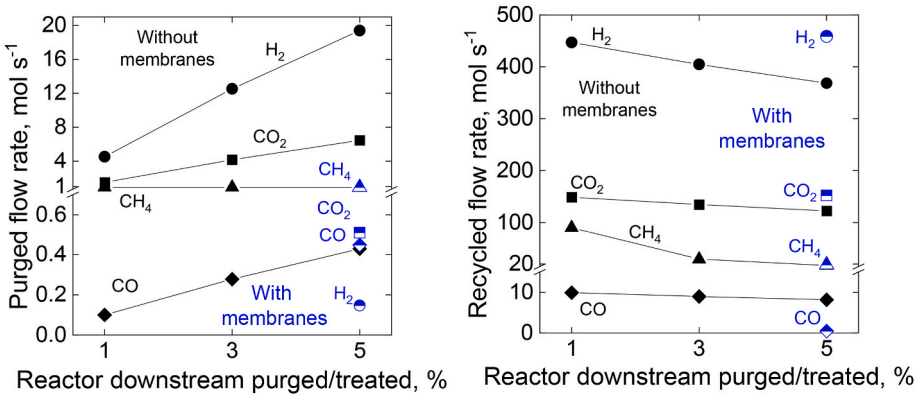

Fig. 8. Recycled flow rates (left side) and purged flow rates (right side) as a function of the reactor gas downstream purged for the scheme without membranes and separated for the scheme with downstream membranes.

the highest values. Therefore, the downstream membrane separation provides a recycled flow rate higher in reactants and lower in CH_4 and CO compared to that obtained with the process without membranes. Overall, the use of membrane separation stage allows to reduce to 0.9% the fraction of reactants lost while effectively removing the species such as CO and CH_4.

The performance of the two integrated processes with and without downstream membrane separation was compared in terms of CO_2 valorisation (Eq. (9)) and H_2 utilisation (Eq. (10)) (Fig. 9). For the configuration without downstream membranes, the CO_2 valorisation attains 0.94 at 1% purge fraction, but decreases markedly to 0.83 at a 5% purge. In contrast, the addition of the downstream membrane separation on purged stream reflects in a higher CO_2 valorisation equal to 0.97. Similarly, hydrogen utilisation for the reference cases decreases from 0.96 to 0.83 as the purge fraction increases, whereas the proposed configuration achieves an almost complete utilisation of the hydrogen fed to the integrated process, reaching a value of 0.999.

The outlet methanol flow rate obtained for the proposed configuration and for the reference cases is shown in Fig. 10. The methanol production decreases with increasing purge fraction, ranging from 37.6 to 32.4 mol s^{-1}. Notably, the addition of membrane separation allows the achievement of a methanol flow rate, equal to 38.3 mol s^{-1}, higher than that obtained in all cases in wich membranes are not included, confirming the benefit of its integration a in the process.

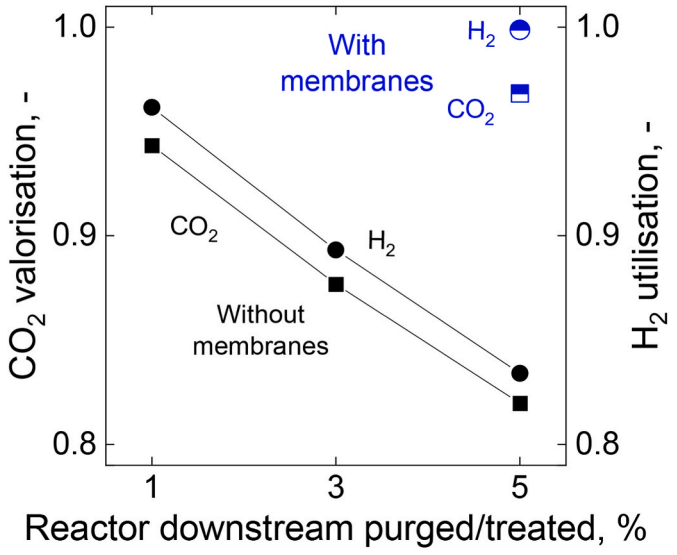

Fig. 9. CO_2 valorisation and H_2 utilisation as a function of the fraction of purged/treated reactor downstream.

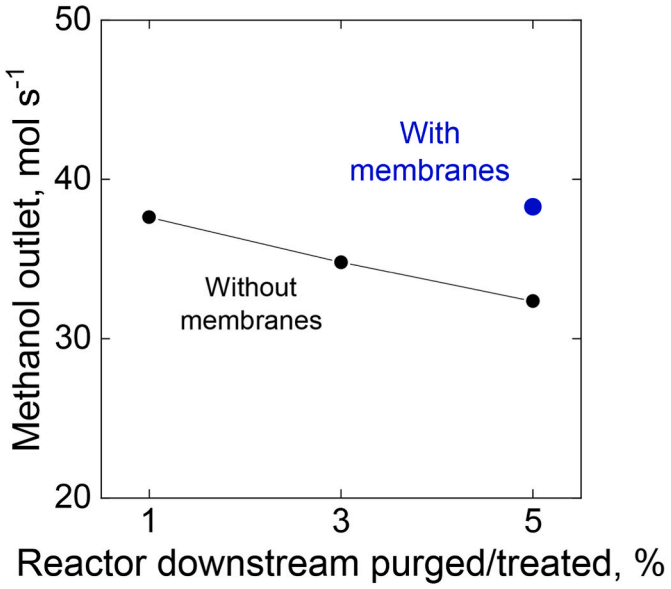

Fig. 10. Methanol outlet flow rate as a function of the fraction of purged/treated reactor downstream.

4. Conclusions

This study presented the design and performance evaluation of a membrane-integrated process for the valorisation of biogas and renewable hydrogen storage through CO_2-to-methanol conversion. The proposed configuration effectively combines gas separation and catalytic conversion steps to maximize CO_2 utilisation and minimize reactant losses.

Upstream of the methanol synthesis reactor, a single-stage membrane section comprising nine separation steps was developed to simultaneously produce a CH_4-rich stream and a CO_2-rich feed for methanol synthesis. The designed configuration achieved a CH_4 recovery of 98.5% at a purity of 98.7%, meeting grid-injection specifications, while producing a CO_2-rich stream with 98.1% recovery and over 97% purity for subsequent conversion.

To further enhance process efficiency, a downstream membrane separation unit was introduced on the reactor purge stream. This four-step unit enabled selective recovery of CO_2 and H_2 for recycling while removing CH_4 and CO. The resulting permeate stream, composed of 75% H_2 and 23% CO_2, was recycled to the reactor inlet, whereas the retentate—mainly CH_4, H_2, and CO—could be valorised to meet process energy demands. Incorporation of this downstream membrane system

reduced the loss of valuable reactants to only 0.9% and substantially improved CO_2 and H_2 utilisation.

Comparative analyses demonstrated that, without downstream membranes, CO_2 valorisation decreased from 0.94 to 0.83 as the purge fraction increased from 1% to 5%. In contrast, the proposed configuration maintained a high CO_2 valorisation of 0.97 and nearly complete hydrogen utilisation. Furthermore, the integration of downstream membrane separation enhanced methanol productivity, achieving an outlet flow rate of 38.3 mol s^{-1}, higher than in all reference cases.

Overall, the dual membrane-integrated design provides a robust and efficient route for biogas upgrading and renewable hydrogen storage via CO_2-to-methanol conversion. The combined upstream and downstream separations ensure optimal reactant recovery, reduced emissions, and improved process sustainability, highlighting the potential of membrane-based integration in power-to-methanol systems.

Nomenclature

$A^{membrane}$	membrane Area, m^2
F	flow rate, mol s^{-1}
L	total membrane length, m
P	Pressure, Pa
X	molar fraction, -
z	membrane length, m
Superscripts	
Feed	feed phase referred to
Grid/Purged	grid/Purged phase referred to
Outlet	outlet phase referred to
Permeate	permeate phase referred to
Retentate	retentate phase referred to
Subscripts	
i, j	component i and component j of the stream

(*continued on next column*)

(*continued*)

Greek letters	
θ	permeation number, -
ϕ	pressure ratio, -
Φ	dimensionless flow rate, -
ζ	dimensionless membrane length, -

CRediT authorship contribution statement

Luigi Marsico: Writing – original draft, Visualization, Validation, Investigation, Data curation. **Adele Brunetti:** Writing – review & editing, Supervision, Methodology, Funding acquisition, Conceptualization. **Enrico Catizzone:** Writing – review & editing, Supervision. **Massimo Migliori:** Supervision. **Giuseppe Barbieri:** Writing – review & editing, Supervision, Methodology, Conceptualization.

Declaration of competing interest

The authors declare that they have no known competing financial interests or personal relationships that could have appeared to influence the work reported in this paper.

Acknowledgements

The authors thank the project "Tech4You—Technologies for climate change adaptation and quality of life improvement"—National Recovery and Resilience Plan (NRRP), Mission 4, Component 2, Investment 1.5, funded from the European Union-NextGenerationEU, Identity code: ECS 00000009, CUP B83C22003980006.

Appendix A. Supplementary data

Supplementary data to this article can be found online at https://doi.org/10.1016/j.ijhydene.2026.153938.

References

[1] Crippa M, Guizzardi D, Pagani F, Banja M, Muntean M, et al. GHG emissions of all world countries - 2025 report. Luxembourg: Publications Office of the European Union; 2025. https://data.europa.eu/doi/10.2760/9816914.

[2] United Nations Environment Programme. Emissions gap report 2024: no more hot air… please! with a massive gap between rhetoric and reality, countries draft new climate commitments, Nairobi. https://doi.org/10.59117/20.500.11822/46404; 2024.

[3] IEA. Global Energy Review 2025. Paris: IEA; 2025. https://www.iea.org/reports/global-energy-review-2025. [Accessed 21 October 2025].

[4] Scarlat N, Dallemand J-F, Fahl F. Biogas: developments and perspectives in Europe. Renew Energy 2018;129:457–72. https://doi.org/10.1016/j.renene.2018.03.006.

[5] Santos-Clotas E, Cabrera-Codony A, Comas J, Martín MJ. Biogas purification through membrane bioreactors: experimental study on siloxane separation and biodegradation. Sep Purif Technol 2020;238:116440. https://doi.org/10.1016/j.seppur.2019.116440.

[6] Awe OW, Zhao Y, Nzihou A, Minh DP, Lyczko N. A review of biogas utilisation, purification and upgrading technologies. Waste Biomass Valor 2017;8:267–83. https://doi.org/10.1007/s12649-016-9826-4.

[7] Pavičić J, Novak Mavar K, Brkić V, Simon K. Biogas and biomethane production and usage: technology development, advantages and challenges in Europe. Energies (Basel) 2022;15:2940. https://doi.org/10.3390/en15082940.

[8] Ryckebosch E, Drouillon M, Vervaeren H. Techniques for transformation of biogas to biomethane. Biomass Bioenergy 2011;35:1633–45. https://doi.org/10.1016/j.biombioe.2011.02.033.

[9] Drioli E, Barbieri G, Brunetti A. Membrane engineering for the treatment of gases –, vol 1. Royal Society of Chemistry; 2017. https://doi.org/10.1039/9781788010443. ISBN: 978-1-78262-875-0.

[10] Bernardo G, Araújo T, da Silva Lopes T, Sousa J, Mendes A. Recent advances in membrane technologies for hydrogen purification. Int J Hydrogen Energy 2020;45:7313–38. https://doi.org/10.1016/j.ijhydene.2019.06.162.

[11] Brunetti A, Barbieri G. Membrane engineering for biogas valorization. Front Chem Eng 2021;3. https://doi.org/10.3389/fceng.2021.775788.

[12] Scholz M, Melin T, Wessling M. Transforming biogas into biomethane using membrane technology. Renew Sustain Energy Rev 2013;17:199–212. https://doi.org/10.1016/j.rser.2012.08.009.

[13] Zito PF, Brunetti A, Barbieri G. Multi-step membrane process for biogas upgrading. J Membr Sci 2022;652:120454. https://doi.org/10.1016/j.memsci.2022.120454.

[14] Gantenbein A, Witte J, Biollaz SMA, Kröcher O, Schildhauer TJ. Flexible application of biogas upgrading membranes for hydrogen recycle in power-to-methane processes. Chem Eng Sci 2021;229:116012. https://doi.org/10.1016/j.ces.2020.116012.

[15] Kirchbacher F, Biegger P, Miltner M, Lehner M, Harasek M. A new methanation and membrane based power-to-gas process for the direct integration of raw biogas – feasability and comparison. Energy 2018;146:34–46. https://doi.org/10.1016/j.energy.2017.05.026.

[16] Marsico L, Brunetti A, Catizzone E, Migliori M, Barbieri G. Integrated membrane gas separation process for the valorisation of H_2 and CO_2 to biomethane. Renew Energy 2025;254:123693. https://doi.org/10.1016/j.renene.2025.123693.

[17] Kim C, Yoo CJ, Oh HS, Min BK, Lee U. Review of carbon dioxide utilization technologies and their potential for industrial application. J CO2 Util 2022;65:102239. https://doi.org/10.1016/j.jcou.2022.102239.

[18] Hong WY. A techno-economic review on carbon capture, utilisation and storage systems for achieving a net-zero CO_2 emissions future. Carbon Capture Sci Technol 2022;3:100044. https://doi.org/10.1016/j.ccst.2022.100044.
[19] Dieterich V, Buttler A, Hanel A, Spliethoff H, Fendt S. Power-to-liquid via synthesis of methanol, DME or Fischer–Tropsch-fuels: a review. Energy Environ Sci 2020;10. https://doi.org/10.1039/D0EE01187H.
[20] Irena and Methanol Institute. Innovation outlook: renewable methanol. Int Renew Energy Agency 2021. Abu Dhabi, [Accessed 21 October 2025].
[21] Leonzio G. State of art and perspectives about the production of methanol, dimethyl ether and syngas by carbon dioxide hydrogenation. J CO2 Util 2018;27: 326–54. https://doi.org/10.1016/j.jcou.2018.08.005.
[22] Sollai S, Porcu A, Tola V, Ferrara F, Pettinau A. Renewable methanol production from green hydrogen and captured CO_2: a techno-economic assessment. J CO2 Util 2023;68:102345. https://doi.org/10.1016/j.jcou.2022.102345.
[23] Renewable methanol plant: first production of fuel from CO_2 at industrial scale. https://carbonrecycling.com/projects/george-olah. [Accessed 21 October 2025].
[24] Cri's largest CO2-to-methanol reactor installed in anyang. https://carbonrecycling.com/about/news/cris-largest-co2-to-methanol-reactor-installed-in-anyang. [Accessed 21 October 2025].
[25] Catizzone E, Bonura G, Migliori M, Frusteri F, Giordano G. CO_2 recycling to dimethyl ether: state of the art. Molecules 2018;23:31. https://doi.org/10.3390/molecules23010031.
[26] Brunetti A, Scura F, Barbieri G, Drioli E. Membrane technologies for CO_2 separation. J Membr Sci 2010;359:115–25. https://doi.org/10.1016/j.memsci.2009.11.040.
[27] Brunetti A, Drioli E, Lee YM, Barbieri G. Engineering evaluation of CO_2 separation by membrane gas separation systems. J Membr Sci 2014;454:305–15. https://doi.org/10.1016/j.memsci.2013.12.037.
[28] Baker RW. Membrane technology and applications. Wiley; 2004. https://doi.org/10.1002/0470020393.
[29] Shahbaz M, Al-Ansari T, Aslam M, Khan Z, Inayat A, Athar M, Naqvi SR, Ahmed MA, McKay G. A state of the art review on biomass processing and conversion technologies to produce hydrogen and its recovery via membrane separation. Int J Hydrogen Energy 2020;45:15166–95. https://doi.org/10.1016/j.ijhydene.2020.04.009.
[30] Yang Y, White MG, Liu P. Theoretical study of methanol synthesis from CO_2 hydrogenation on metal-doped Cu(111) surfaces. J Phys Chem C 2011;116: 248–56.
[31] Giglio E, Bianco M, Zanardi G, Catizzone E, Giordano G, Migliori M. Direct biogas methanation via renewable-based Power-to-Gas: techno-economic assessment based on real industrial data. Energy Convers Manag 2025;332:119775. https://doi.org/10.1016/j.enconman.2025.119775.
[32] Heydorn EC, Diamond BW, Lilly RD. Commercial-scale demonstration of the liquid phase methanol (LPMEOH) process. U.S. Department of Energy; 2003. Final Report (Volume 2: Project Performance and Economics).
[33] Lacerda de Oliveira Campos B, John K, Beeskow P, Herrera Delgado K, Pitter S, Dahmen N, Sauer J. A detailed process and techno-economic analysis of methanol synthesis from H_2 and CO_2 with intermediate condensation steps. Processes 2022; 10–8:1535. https://doi.org/10.3390/pr10081535.
[34] Khalilpourmeymandi H, Mirvakili A, Rahimpour MR, Shariati A. Application of response surface methodology for optimization of purge gas recycling to an industrial reactor for conversion of CO_2 to methanol. Chin J Chem Eng 2017;25–5: 676–87. https://doi.org/10.1016/j.cjche.2016.10.020.